First Principles Modeling for Research and Design of New Materials

G. Ceder
Department of Materials Science and Engineering
Massachusetts Institute of Technology, Cambridge MA 02139

First principles computation can be used to investigate an design materials in ways that can not be achieved with experimental means. We show how computations can be used to rapidly capture the essential physics that determines the useful properties in different applications. Some applications for predicting crystal structure, thermodynamic and kinetic properties, and phase stability are discussed. This first principles tool set will be demonstrated with applications from rechargeable batteries and hydrogen storage materials.

Similar to how an architect draws the plan for a house, it should be possible to design a new material completely on paper, optimizing the composition and processing steps in order to achieve the properties required for a given application. In principle, this is possible, as all the properties of a material are determined by the constituent atoms and the basic laws of physics. This promise, of atomic-scale engineering of materials properties, is the driving force for the tremendous growth of atomistic materials modeling. In particular, first-principles or ab-initio calculations, where all basic data is derived from quantum mechanics holds great promise as it requires no experimental input on a material. While it may seem odd to go to quantum mechanics to engineer materials, the dramatic progress of the last twenty years in solving the Schrödinger equation, and the availability of user-friendly programs, has commoditized quantum mechanics and brought its opportunities square into materials science and engineering.

The ability to compute properties of matter from scratch brings obvious advantages to materials research. By predicting the properties of a series of materials before they are synthesized, computational modeling can guide experiments in promising directions, and (just as importantly) steer it away from attempts that would be less fruitful. Experimental guidance can come from either the specific interesting materials that are called out by a calculation, or from the insight gained by it. Gaining insight through modeling is facilitated by the control it offers. A material studied in a calculation is always perfectly characterized in terms of structure, composition, defects etc. This makes the results of computations often less ambiguous than in experiments, where the characterization in terms of its (micro)structure, composition, defects etc. is often incomplete. In essence, modeling gives approximate answers to exactly characterized materials, whereas experiments gives exact (in the sense of "true") answers to approximately characterized materials. This detailed control in computations can be used to rapidly gain insight into the factors that influence a particular property of materials. In this paper we demonstrate this with applications to materials for lithium batteries and for hydrogen storage.

Rechargeable lithium batteries are responsible for about 11% of U.S. Li consumption, well behind the aluminum and glass industry. The growth potential of this market is however very large. In Japan, Li batteries have already overtaken the competing Nickel-Cadmium(Ni-Cd) and Nickel-metal-hydride(NiM-H) technologies in sales volume. With Nickel-metal-hydride and Ni-Cd sales flat it is expected that Li technology will capture the high-end of the battery market and progressively move down to lower-cost applications. The market for rechargeable lithium batteries is expected to reach $10 billion by the year 2003.

The popularity of rechargeable lithium batteries stems from their high energy densities. Currently all large manufacturers of Li batteries (Sony, Sanyo, Matsushita, AT Battery) use $LiCoO_2$ as the cathode material. The high price of Co has spurred considerable interest in cathode-oxides based on less expensive (and more environmentally benign) transition metals. One of these, $LiMn_2O_4$, is currently making its entry into the marketplace, although it does not deliver the energy density of $LiCoO_2$. Several other 3d-metal oxides are also being investigated for application in rechargeable lithium batteries.

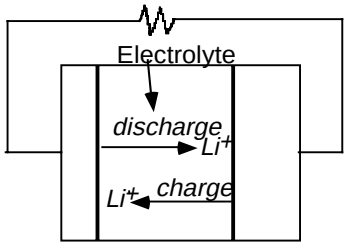

Figure 1: Working of a rechargeable Li battery

Figure 1 shows schematically the operation of a rechargeable Li battery . The equilibrium cell voltage is directly proportional to the lithium chemical potential difference in the anode and cathode:

$$E = -\frac{\mu_{Li}^{cathode} - \mu_{Li}^{anode}}{F} \qquad (1)$$

F is the Faraday constant. By using electrode materials for which the chemical potential is very different (e.g. lithium-oxides versus metallic lithium) a single-cell voltage of 3.6 - 4V can be obtained in a typical commercial Li battery. Upon discharge Li^+ ions are transported through the electrolyte (typically an organic solvent based on diethyl carbonate, ethyl carbonate or propylene carbonate, plus $LiPF_6$ salt) to the cathode where they intercalate into the crystal structure of a host material such as Li_xCoO_2. $LiCoO_2$, which corresponds to the fully discharged cathode, has an ordered rocksalt structure ($R\bar{3}m$) in which Co and Li planes

alternate between close-packed oxygen layers. As the battery is charged Li ions are removed from these planes leaving vacancies behind.

Substantial battery capacity requires a cathode host which can accommodate both Li^+ ions and electrons with minimal structural changes. While the Li^+ ion intercalates into empty sites of the crystal structure, the electron is transferred to the components of the host material (as lithium typically remains ionized in the oxide). While the combination of high voltage and capacity leads to high energy density, it is the retention of this capacity upon cycling that is one of the most difficult problems in rechargeable battery technology. Most batteries show some loss after repeated charge/discharge cycles.

As is common in materials development, the design of active cathode oxides has so far been largely done empirically. While this may ultimately lead to materials with good performance, we indicate how this process can be shortened with modern computational modeling tools. In the rest of this paper, it is demonstrated that first-principles calculations can actually *predict* several of the important properties of new intercalation oxides with modified composition or structure. Figure 2 shows the voltages predicted from first principles for a large series of transition metal oxides. This computational approach allow one to scan quickly over a large set of compositions and structures and select those that look promising for further investigation.

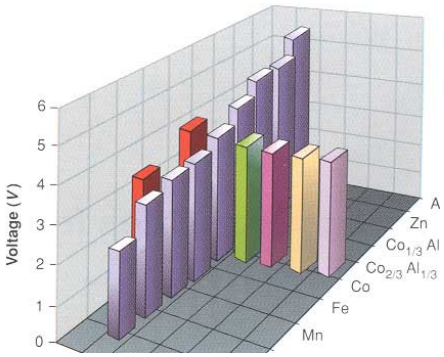

One of the problems has been to find a substitute for $LiCoO_2$. Co is expensive and at high levels of charge.the materials prone to decomposition. In particular in large battery assemblies, as for example in cars, thermal management of the battery system is therefore difficult. The search for safer and less costly materials has been extensive. Ni, Mn, Fe and Mn based oxides have been targeted in particular.

Layered lithium-manganese oxides are of interest for use in rechargeable lithium batteries, because of their potential for very high capacity, while being relatively safe and inexpensive. Their inherent safety is derived from the fact that both Mn^{3+} (present at the end of discharge) and Mn^{4+} (at the end of charge) are quite stable valence states. While manganese oxides with the spinel structure and stoichiometry $LiMn_2O_4$ have been used in batteries, their capacity is limited, and severe stability issues exist with the material. Layered lithium manganese oxides on the other hand have a theoretical capacity of 288 mAh/g. Unfortunately, the layered α-$NaFeO_2$ structure is not the ground state for $LiMnO_2$[1] and hence one has had to resort to either metastable processing routes [2, 3] starting from a $NaMnO_2$, or to compositional modifications in order to increase the stability of the layered phase over the other possible polytopes [4, 5, 6, 7]. Almost all of the pure or lightly doped layered manganese oxides have shown a rapid transformation to a spinel upon cycling [8, 9]. While this spinel can in some cases maintain capacity [10], it has a less favorable voltage profile and the remaining disorder in the structure limits its current density.

Using higher doping levels, it has been possible to stabilize the layered structure against transformation to spinel. In particular co-doping of Li and Cr [5, 11] has been particularly successful. Ni-doped Mn materials have been synthesized several years ago [12, 13], but this approach has gained renewed interest now that good cycling behavior for these materials has been demonstrated [5, 14].

Some uncertainty exists with regards to the valence states in these mixed-metal compounds. In $Li(Li,Cr,Mn)O_2$ the observed capacity could only be explained by the cycling of Cr^{3+} to Cr^{6+} [5], a fact later confirmed with X-ray absorption spectroscopy [15]. In $LiNi_{0.5}Mn_{0.5}O_2$ it has been speculated [5, 14] that the Ni and Mn ions respectively have valence +2 and +4, though earlier work by Spahr [13] assumed both Ni and Mn to have valence +3 in the starting material. Since the capacity of $LiNi_{0.5}Mn_{0.5}O_2$ is > 200mAh/g the assumption of Ni^{2+} and Mn^{4+} in the starting material requires that the nickel ion cycles between Ni^{2+} and Ni^{4+}. The purpose of this paper is to clarify the valence states in $LiNi_{0.5}Mn_{0.5}O_2$ and characterize the electronic and structural changes that occur upon delithiation. The origin for the high potential of this material will also be discussed. The energies, intercalation potentials, geometries and electronic structure of the $Li_xNi_{0.5}Mn_{0.5}O_2$ materials are obtained using first principles quantum mechanical computations in the Generalized Gradient Approximation to Density Functional Theory. Ultrasoft pseudopotentials and the Perdew-Wang exchange correlation function were used, as implemented in VASP [16]. All calculations were performed with spin polarization, previously demonstrated to be crucial in manganese oxides [1]. Reasonable intercalation potentials and geometrical information can be obtained with first principles methods, as has been amply demonstrated [17, 18, 19]. To describe the $LiNi_{0.5}Mn_{0.5}O_2$ system, a supercell with two formula units was used. Because this computational approach (as do most computational methods) requires the use of periodic cells, the Mn and Ni are long-range ordered in rows on the triangular lattice of transition metal sites. In all cells the symmetry was lowered enough (lower than given by the relevant Li/vacancy or Ni/Mn) so that Jahn-Teller distortions could take place if

energetically favorable. Practically, this means that the symmetry is always a subgroup of the C2/m group of the monoclinic layered $LiMnO_2$.

The valence state of a high-spin transition metal ion can best be determined by integrating the spin-polarization density in a sphere around the ion. Using spin density is much more effective than integrating the charge density, as the former allows to filter out the contribution from the oxygen *p*-states which usually carry very little net electron spin. For the relevant ions , Mn^{4+}, Mn^{3+} and Mn^{2+}, we expect respectively a total electron spin count of 3, 4 and 5 (in units of 1/2 μ_B). For Ni^{4+}, Ni^{3+} and Ni^{2+} we expect 0, 1 and 2 electron spins as the Ni^{4+} has a core of non-spin polarized filled t_{2g} levels. Figure 3 shows the integrated spin as function of integration radius around Ni and Mn in the $LiNi_{0.5}Mn_{0.5}O_2$ structure. The integrated moment increases steeply as we integrate through the d-states of the metal ion, but then reaches a plateau value since the charge density of the oxygen ions does not contribute to the spin density. After this plateau the integrated value increases again as spin from neighboring transition metals is picked up. The Mn ion in $LiNi_{0.5}Mn_{0.5}O_2$ clearly carries 3 electrons, corresponding to a valence of Mn^{4+}. The moment around Ni is slightly below what is expected for Ni^{2+}.

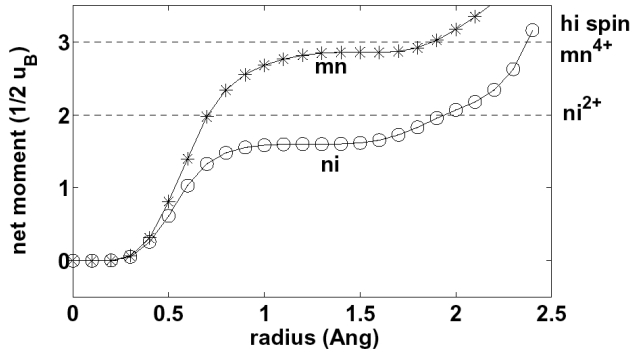

Figure 3: Integrated spin density around Ni and Mn in $Li(Ni,Mn)O_2$.

The remainder of the moment is probably on the oxygen ions as is typical for nickel oxides. Some evidence for this lies in the fact that the point where the integrated spin density rises from the plateau value is at a shorter radius than for the Mn^{4+} ion. The spin integration in Figure 13 indicates that the formal valence states are $LiNi_{0.5}{}^{II}Mn_{0.5}{}^{IV}O_2$. Further evidence can be found from the changes in spin density upon lithium removal. Figure 4 shows similar spin integrations for the delithiated material $Ni_{0.5}Mn_{0.5}O_2$. The spin on Mn is barely different from what it is in the fully lithiated material, while Ni has lost most of its moment, consistent with the electron configuration for Ni^{4+} in $Ni_{0.5}Mn_{0.5}O_2$. Figure 3 and 4 offer strong evidence that in $LiNi_{0.5}Mn_{0.5}O_2$ the correct valence assignment is $Ni^{2+}$and Mn^{4+}. Upon Li removal Ni^2 is oxidized to Ni^{4+} while the Mn^{4+} ion remains unchanged.

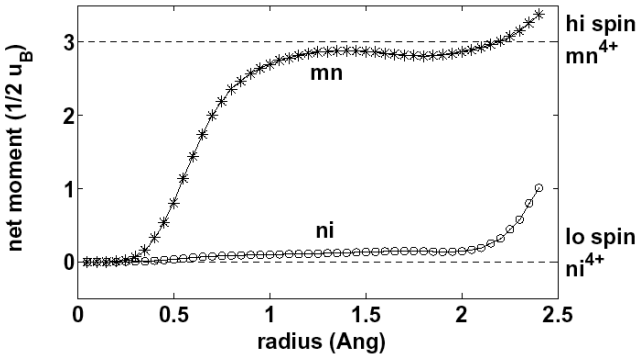

Figure 4: Spin density in $(Ni,Mn)O_2$

We have also calculated the average discharge potential for the system $LiNi_{0.5}Mn_{0.5}O_2$/ $Ni_{0.5}Mn_{0.5}O_2$. These are compared to experiment in Table 2. The calculated potentials are below the experimental values as is typical with standard first principles energy methods[17]. Hence, to make a better prediction possible, we have estimated a correction based on the difference between measured and calculated potentials for $LiNiO_2$. This correction (+ 0.73 V) is added to the calculated potential to give the result in the last column. We emphasize that this adjustment is purely phenomenological and for the purpose of facilitating the direct comparison with experiments for $LiNi_{0.5}Mn_{0.5}O_2$. The data in this column agrees well with the measured values for $LiNi_{0.5}Mn_{0.5}O_2$. In the last row of the table the potential is broken down into the average for the interval $LiNi_{0.5}Mn_{0.5}O_2$ to $Li_{0.5}Ni_{0.5}Mn_{0.5}O_2$, and $Li_{0.5}Ni_{0.5}Mn_{0.5}O_2$ to $Ni_{0.5}Mn_{0.5}O_2$. Some indication of the variation of potential upon charge can be derived form this.

	Calculated		Exp.	Adjusted	
$LiNiO_2$	3.17		3.9 [28]	3.9	
$LiNi_{0.5}Mn_{0.5}O_2$	3.22		3.9 [14]	3.95	
$LiNi_{0.5}Mn_{0.5}O_2$	$0.5 < x_{li} < 1$	$x_{li} < 0.5$		$0.5 < x_{li} < 1$	$0 < x_{li} < 0.5$
	2.94	3.51		3.67	4.24

Table 2: Comparison between calculated and measured average discharge potentials for the $LiNi_{0.5}Mn_{0.5}O_2$ and $LiNiO_2$ systems. The last column includes a correction to the computed voltage based on the difference between calculation and

Table 2 highlights the fact that the potential of $LiNi_{0.5}Mn_{0.5}O_2$ is actually very close to that of $LiNiO_2$. This is surprising since our results indicate that different redox couples are active in both materials. In $LiNiO_2$ only Ni^{3+}/Ni^{4+} is active, while both Ni^{2+}/Ni^{3+} and Ni^{3+}/Ni^{4+} occur in $LiNi_{0.5}Mn_{0.5}O_2$. Hence the average potential for $LiNi_{0.5}Mn_{0.5}O_2$ should be lower than for $LiNiO_2$. Even if one believed that Mn participates in the redox process the higher potential is difficult to explain, since the Mn^{3+}/Mn^{4+} couple is

below that of Ni^{3+}/Ni^{4+}. These experimental and theoretical results are further evidence that strong interactions exist between the redox couples of metals when they are mixed[23]. In general alloy theory [24] a measure of the effective Ni-Mn interactions can be obtained by comparing the energy of $LiNi_{0.5}Mn_{0.5}O_2$ to the average energy of $LiNiO_2$ and $LiMnO_2$. If $\Delta \mathbf{E}_{mix} \equiv \mathbf{E}(LiNi_{0.5}Mn_{0.5}O_2) - 1/2 [\mathbf{E}(LiNiO_2) + \mathbf{E}(LiMnO_2)]$ is negative, Ni and Mn have an effective attractive interaction and the system will be either randomly mixed or ordered, depending on the strength of the interaction and the preparation temperature. If $\Delta \mathbf{E}_{mix}$ is positive, local phase separation into Mn and Ni rich regions is energetically preferred, though random mixing may be achieved if the synthesis temperature is high enough. From calculting the relevant energy numbers in the above equation we find that for $LiNi_{0.5}Mn_{0.5}O_2$ $\Delta \mathbf{E}_{mix}$ is –216 meV per formula unit, indicating a strong ordering (attractive) tendency between Ni and Mn. Similarly, for the delithiated material $\Delta \mathbf{E}_{mix} = \mathbf{E}(Ni_{0.5}Mn_{0.5}O_2) - 1/2 [\mathbf{E}(NiO_2) + \mathbf{E}(MnO_2)]$ is computed to be + 50 meV, indicating repulsive Ni-Mn interactions. These results give some insight as to why the voltage is higher than may be expected for this system. Ni-Mn interactions go from being attractive in $LiNi_{0.5}Mn_{0.5}O_2$ to being repulsive in $Ni_{0.5}Mn_{0.5}O_2$. Hence, to remove lithium one not only has to supply the binding energy for the Li ion and electron, but also the strong energy increase in the system due to the Mn-Ni bonds becoming unfavorable (as that interaction turns from attractive to repulsive). It can be easily deduced that the effect of changes in the metal-metal interactions upon the average discharge potential is given by the following equation:

$$\Delta\phi = \Delta\mathbf{E}_{mix}(X_{Li}=1) - \Delta\mathbf{E}_{mix}(X_{Li}=0),$$

where ϕ is the equilibrium potential over the range $0 < x_{Li} < 1$. For the $LiNi_{0.5}Mn_{0.5}O_2$ system, this result indicates that the potential is raised by about 266 mV over what would be expected if no Ni-Mn interactions were present (e.g. if Ni^{2+}/Ni^{4+} acted in a pure host, without the presence of Mn). These numbers are derived from calculations on an ordered supercell of Ni and Mn. We have estimated that if the Ni and Mn ions were fully randomized (rather than ordered in the supercell that we used for the calculations) the increase in potential would be slightly less and about 200 mV.

The effect of Li on the Ni-Mn interactions can be easily understood, using what is known about the miscibility of oxides [25]. The effective interaction, for studying phase stability and mixing is not the bare ionic interaction but the energy difference between the average of identical pairs (i.e. Ni-Ni and Mn-Mn) and different pairs (i.e. Ni-Mn). Hence the simplest way to sample this difference is to consider the difference in energy between $LiNi_{0.5}Mn_{0.5}O_2$ (where Ni-Mn bonds are present) and $LiNiO_2$ (with Ni-Ni bonds) and $LiMnO_2$ (with Mn-Mn bonds). In the delithiated state, Ni and Mn have the same +4 valence and there is no net electrostatic interaction for exchanging their positions. It can be easily shown that for such iso-valent ions, the net interaction is due to size effects, and is always repulsive [26]. This agrees with our result of a positive mixing energy in the delithiated state. On the other hand, in the lithiated material the different valence of Ni and Mn leads to a strong effective attractive interaction and hence explains the ordering or mixing tendency.

Our results conclusively indicate that in $LiNi_{0.5}Mn_{0.5}O_2$ (and hence in the related systems $Li[Ni_xLi_{(1/3-2x/3)}Mn_{(2/3-x/3)}]O_2$ [14] Ni is the electrochemically active ion and cycles between Ni^{2+} and Ni^{4}. The material remains kinetically stable against transformation to spinel because Mn is not present in oxidation states lower than +4. We recently showed [27] that the very rapid transformation of layered $LiMnO_2$ to spinel is due to the ease with which Mn^{3+} disproportionates to Mn^{2+} and Mn^{4+}. This allows Mn to rapidly migrate through tetrahedral sites as Mn^{2+}. Mn^{4+} on the other hand, was shown to have a very high activation barrier for diffusion through the tetrahedral site. Hence, layered oxides with only manganese in the 4+ oxidation state are expected to be quite stable. In cycling between $LiNi_{0.5}Mn_{0.5}O_2$ and $Ni_{0.5}Mn_{0.5}O_2$ the Ni-Mn arrangement remains fixed due the lack of any transition metal mobility at room temperature, but the interactions between the ions change considerably. In this system, this change in Ni-Mn interactions causes to increase the voltage fo the Ni^{2+}/Ni^{4} couple over what it would be in a non-interacting matrix.

The class of materials in which the valence of Ni is +2 and Mn is +4 seems to possess many desirable features for a cathode material. They also point at new and interesting directions for cathode research. The combination of experimental data on highly doped systems and our understanding of the role of Mn^{3+} in the problems of many Mn-oxides clearly indicate that stable layered Mn oxides, containing only Mn^{4+} can be made. In those material Mn has given up its role as electrochemically active center and only is present as "filler". Hence, other metals, selected on the basis of cost, weight, processability, environmental behavior etc., could be selected to substitute for Mn.

Clearly, first principles calculations can be useful for investigating and designing new materials.

Acknowledgments:

The authors would like to acknowledge the support from Singapore MIT Alliance

References

1. S. K. Mishra, G. Ceder, *Physical Review B* **59**, (1999) 6120-6130.
2. F. Capitaine, P. Gravereau, C. Delmas, *Solid State Ionics, Diffusion & Reactions* **89**, (1996) 197-202.
3. A. R. Armstrong, P. G. Bruce, *Nature* **381**, (1996) 499-500.
4. I. J. Davidson, R. S. McMillan, H. Slegr, B. Luan, I. Kargina, J. J. Murray, I. P. Swainson, *Journal of Power Sources* **82**, (1999) 406-411.
5. B. Ammundsen, J. Paulsen, *Advanced Materials* **13**, (2001) 943-956.
6. Y.-I. Jang, B. Huang, Y.-M. Chiang, D. R. Sadoway, *Electrochemical and Solid State Letters* **1**, (1998) 13-16.
7. B. Ammundsen, J. Desilvestro, T. Groutso, D. Hassell, J. B. Metson, E. Regan, R. Steiner, P. J. Pickering, *Journal of the Electrochemical Society* **147**, (2000) 4078-82.
8. H. Wang, Y.-I. Jang, Y.-M. Chiang, *Mat. Res. Soc. Symp. Proc, submitted* , (1998) .
9. Y. Shao-Horn, S. A. Hackney, A. R. Armstrong, P. G. Bruce, Gitzendanner, C. S. Johnson, M. M. Thackeray, *J. Electrochem. Soc.* **146**, (1999) 2404-2412.
10. Y.-M. Chiang, D. R. Sadoway, Y.-I. Jang, B. Huang, H. Wang, *Electrochem. Sol. St. Lett* **2**, (1999) 107-110.
11. C. Storey, I. Kargina, Y. Grincourt, I. J. Davidson, Y. C. Yoo, D. Y. Seung, *Journal of Power Sources* **97-98**, (2001) 541-544.
12. E. Rossen, C. D. W. Jones, J. R. Dahn, *Solid State Ionics* **57**, (1992) 311.
13. M. E. Spahr, P. Novak, B. Schneyder, O. Haas, R. Nesper, *J. Electrochem. Soc.* **145**, (1998) 1113-1121.
14. Z. Lu, D. D. MacNeil, J. R. Dahn, *Electrochemical and Solid State Letters* **4**, (2001) A191-A194.
15. B. Ammundsen, J. M. Paulsen, I. J. Davidson, *unpublished* , (2001) .
16. G. Kresse, J. Furthmüller, *Comput. Mat. Sci.* **6**, (1996) 15-50.
17. M. K. Aydinol, A. F. Kohan, G. Ceder, K. Cho, J. Joannopoulos, *Phys. Rev. B* **56**, (1997) 1354-1365.
18. A. Van der Ven, M. K. Aydinol, G. Ceder, G. Kresse, J. Hafner, *Phys. Rev. B* **58**, (1998) 2975-2987.
19. C. Wolverton, A. Zunger, *Physical Review Letters* **81**, (1998) 606-609.
20. A. N. Mansour, X. Q. Yang, X. Sun, J. McBreen, L. Croguennec, C. Delmas, *J. of Electrochem Soc.* **147**, (2000) 2104-2109.
21. L. Croguennec, C. Pouillerle, C. Delmas, *J. Electrochem. Soc.* **147**, (2000) 1314-21.
22. C. A. Marianetti, D. Morgan, G. Ceder, *Phys. Rev. B* **63**, (2001) 224304/1-15.
23. G. Ceder, Y.-M. Chiang, D. R. Sadoway, M. K. Aydinol, Y.-I. Jang, B. Huang, *Nature* **392**, (1998) 694-696.
24. D. de Fontaine, in *Solid State Physics* H. Ehrenreich, D. Turnbull, Eds. (Academic Press, 1994), vol. 47, pp. 33-176.
25. G. Ceder, A. Van der Ven, C. Marianetti, D. Morgan, *Modeling and Simulation in Materials Science and Engineering* **8**, (2000) 311-321.
26. P. D. Tepesch, A. F. Kohan, G. D. Garbulsky, G. Ceder, C. Coley, H. T. Stokes, L. L. Boyer, M. J. Mehl, B. Burton, K. Cho, J. Joannopoulos, *J. Am. Ceram. Soc.* **79**, (1996) 2033-2040.
27. J. Reed, A. Van der Ven, G. Ceder, *Electrochemical and Solid State Letters* **4**, (2001) A78-A81.
28. C. Delmas, J. P. Peres, A. Rougier, A. Demourgues, F. Weill, A. Chadwick, M. Broussely, F. Perton, P. Biensan, P. Willmann, *Journal of Power Sources* **68**, (1997) 120-125.